

Copper(II) Complexes of N-Octylated Bis(benzimidazole) Diamide Ligands and Their Peroxide-Dependent Oxidation of Aryl Alcohols

Sarita Tehlan,[†] M. S. Hundal,[‡] and Pavan Mathur^{*†}

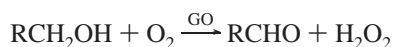
Departments of Chemistry, University of Delhi, Delhi-110007, India, and Gurunanak Dev University, Amritsar, India

Received October 2, 2003

New N-octylated benzimidazole-based diamide ligands *N,N*-bis(*N*-octylbenzimidazolyl-2-ethyl)hexanediamide (O-ABHA), possessing a chiral center, and *N,N*-bis(*N*-octylbenzimidazolyl-2-methyl)hexanediamide (O-GBHA) have been synthesized and utilized to prepare Cu(II) complexes of general composition [Cu(L)X]X, where L = O-ABHA or O-GBHA and X = Cl⁻ or NO₃⁻. The X-ray structure of one of the complexes, [Cu(O-GBHA)NO₃]NO₃, has been obtained. The Cu(II) ion is found to possess a distorted octahedral geometry with a highly unsymmetrical bidentate nitrate group. The N₂O₂ equatorial plane comprises an amide carbonyl O, a nitrate O, and the two benzimidazole imine N atoms while another amide carbonyl O and nitrate O take up the axial positions. The complexes carry out the oxidation of aromatic alcohols to aldehydes in the presence of cumenyl hydroperoxide at 40–45 °C and act as catalyst with turnovers varying between 13- and 27-fold. The percentage yields of the respective products have been obtained which vary from 32% to 65% with respect to the catalyst turnover.

Introduction

Galactose oxidase (GO) is a fungal enzyme containing mononuclear copper ion, which catalyzes the oxidation of primary alcohols to aldehydes, coupled to the two electron reduction of O₂ to H₂O₂.¹



In its catalytic cycle, a unique tyrosyl radical cofactor plays a vital role.² The Cu(II) is located in a distorted square-based pyramidal environment with a tyrosine-495 in the apical position; the amino acids Try-272, His-496, and His-581 and an acetate ion form the N₂O₂ square planar geometry around the Cu(II) site.³ Reaction with one-electron oxidants such as [Fe(CN)₆]³⁻ (or IrCl₆²⁻) is sufficient for the enzyme to become active⁴ in the absence of O₂.

Earlier a large number of phenolate-based Cu(II) complexes have been reported as structural models,⁷ of which only a few mononuclear copper(II) complexes have been reported that act as functional mimics of galactose oxidase. These complexes catalyze the aerobic oxidation of primary alcohols to aldehydes.^{5,6} Reports of functional mimics of galactose oxidase activity with non-phenolate-based ligands are scarce to the best of our knowledge.

We have initiated a study of new bis(benzimidazole)-based diamide ligands, where the bound copper(II) is in a distorted five-coordinate environment with anodic *E*_{1/2} values.⁸ The present series of tetradentate diamide ligands *N,N'*-bis(*N*-octyl-2-benzimidazolylethyl)hexanediamide (O-ABHA) and *N,N'*-bis(*N*-octyl-2-benzimidazolylmethyl)hexanediamide (O-GBHA) and their copper(II) complexes are being reported for the first time. These have been found to carry out

* Author to whom correspondence should be addressed. E-mail: pavanmat@yahoo.co.in.

[†] University of Delhi.

[‡] Gurunanak Dev University.

- (1) (a) Klinman, J. P. *Chem. Rev.* **1996**, *96*, 2541. (b) Whittaker, J. W.; Whittaker, M. M. *Pure Appl. Chem.* **1998**, *70*, 903. (c) Whittaker, J. W.; Sigel, H.; Sigel, A. *Met. Ions Biol. Syst.* **1994**, *30*, 315.
- (2) Whittaker, M. M.; De Vito, V. L.; Asher, S. A.; Whittaker, J. W. *J. Biol. Chem.* **1989**, *264*, 7104.
- (3) (a) Ito N.; Phillips, S. E. V.; Stevens, C.; Ogel, Z. B.; McPherson, M. J.; Keen, J. N.; Yadav, K. D. S.; Knowles, P. F. *Nature* **1991**, *350*, 87. (b) Ito N.; Phillips, S. E. V.; Yadav, K. D. S.; Knowles, P. F. *J. Mol. Biol.* **1994**, *238*, 794.

- (4) Whittaker, M. M.; Whittaker, J. W. *J. Biol. Chem.* **1988**, *263*, 6074.
- (5) (a) Wang, Y.; Stack, T. D. P. *J. Am. Chem. Soc.* **1996**, *118*, 13097 (b) Wang, Y.; Du Bois, J. L.; Hedman, B.; Hodgson, K. O.; Stack, T. D. P. *Science* **1998**, *279*, 537.
- (6) (a) Chaudhuri, P.; Hess, M.; Flörke, U.; Wieghardt, K. *Angew. Chem., Int. Ed.* **1999**, *38*, 1095. (b) Chaudhuri, P.; Hess, M.; Miller, J.; Hildenbrand, K.; Bill, E.; Weyhermüller, T.; Wieghardt, K. *J. Am. Chem. Soc.* **1999**, *121*, 9599.
- (7) (a) Miller, J.; Weyhermüller, T.; Bill, E.; Hildebrandt, O.; Ould Maussa, L.; Glaser, T.; Wieghardt, K. *Angew. Chem., Int. Ed.* **1998**, *37*, 616. (b) Halcrow, M. A.; Chia, L. M. L.; Liu, X.; McInnes, J. L.; Yellow Less, L. J.; Makbs, F. E.; Davies, J. E. *Chem. Commun.* **1998**, 2465.
- (8) Gupta, M.; Mathur, P.; Butcher, R. J. *Inorg. Chem.* **2001**, *40*, 878.

peroxide-dependent facile oxidation of the aryl alcohols to aldehydes, a function similar to that of galactose oxidase.

Experimental Section

Materials. 2-(α -Aminoethyl)benzimidazole dihydrochloride and glycine benzimidazole dihydrochloride were prepared by following the procedure reported by Cescon and Day.⁹ Solvents of spectroscopic grade were used for HPLC purpose, and the rest were freshly distilled off before use. Other chemicals were obtained from commercial sources and used as such.

Physical Measurements. Elemental analyses were obtained from the microanalytical laboratories of RSIC, Chandigarh, India, and University of Delhi, Delhi, India. Electronic spectra were recorded on a Shimadzu 1601 UV-vis spectrophotometer. IR spectra were recorded in the solid state as KBr pellets on a Perkin-Elmer FTIR-2002 spectrometer (accuracy of $\pm 1 \text{ cm}^{-1}$).

¹H NMR spectra were recorded on a 300 MHz Bruker-spin instrument. Magnetic susceptibility measurements were done in CDCl₃ on a 300 MHz Bruker-spin instrument. HPLC was performed on a Waters HPLC with Water 991 photodiode and array detector. Cyclic voltammetric measurements were carried out on a BAS CV 50 W electrochemical analyzing system (accuracy $\pm 1.0 \text{ mV}$). Cyclic voltammograms were recorded in CH₂Cl₂ with 0.1 M TBAP as supporting electrolyte and glassy carbon as the working electrode.

X-ray Data Collection, Structure Determination, and Refinement. The crystal quality was not very good because they were air sensitive. The data were collected after dipping a crystal in crystallographic oil. A number of crystals were tried. The final data set used has $R_{\text{int}} = 0.1544$, indicating low quality data, but it is the best out of the available sets. The intensity data were collected on a Siemens P4 single-crystal diffractometer, up to $2\theta = 55^\circ$, by using the 2θ scanning mode with graphite-monochromatized Mo K α radiation ($\lambda = 0.71073 \text{ \AA}$), on a $0.2 \times 0.1 \times 0.1 \text{ mm}$ crystal at 293 K. A total of 10 043 reflections were measured, and 9574 were independent of which only 2598 [$I > 2\sigma(I)$] were considered observed. Data were corrected for Lorentz and polarization effects. An absorption correction was applied using a ψ scan. The crystal data and refinement parameters are shown in Table 1. The structure was solved by direct methods using SIR92¹⁰ and refined by full-matrix least-squares refinement techniques on F^2 using SHELXL-PC.¹¹ The two octyl chains showed disorder in some of their carbon atoms, as revealed by their having abnormal bond distances and high thermal parameters. Each of these carbon atoms was split into two atomic positions with total site occupancy of 1.0 and refined isotropically having one thermal parameter each for a pair, as free variables. But the disorder could be resolved for only four methylene carbons C27, C28, C29, and C36 and one methyl carbon C38 from these two chains. These five atoms were then assigned the refined site occupancies and were treated isotropically with restrained C–C bond length of 1.510(2) \AA and C–C (nonbonding) of 2.10(2) \AA in the subsequent refinements. All other non-hydrogen atoms were refined anisotropically. The hydrogens were fixed geometrically as riding atoms with a displacement parameter equal to 1.2 (CH, CH₂) or 1.5 (CH₃) times that of the parent atom. The final refinement gave $R_1 = 0.1315$ and $wR_2 = 0.2694$ for observed reflections, $R_1 = 0.3614$ and $wR_2 = 0.3542$ for all reflections, 487 parameters, and 21 restraints. The final R value is on the higher

Table 1. Summary of Crystallographic Data for Compound [Cu(O-GBHA)(NO₃)](NO₃)

empirical formula	C ₃₈ H ₅₆ N ₈ O ₈ Cu
fw	816.45
temp, K	293(2)
wavelength, \AA	0.71069
cryst system, space group	monoclinic, $P2_1/n$
a , \AA	12.935(5)
b , \AA	19.419(5)
c , \AA	16.677(5)
α , deg	90
β , deg	95.590(5)
γ , deg	90
V , \AA^3	4169(2)
Z	4
ρ_{calcd} , Mg m^{-3}	1.301
θ , deg	1.61–27.52
μ , mm^{-1}	0.582
$F(000)$	1732
final R indices ^a	$R_1 = 0.1315$
[$I > 2\sigma(I)$]	$wR_2 = 0.2694$
R indices (all data) ^a	$R_1 = 0.3614$
	$wR_2 = 0.3542$
extinction coeff	0.016(2)

$$^a R_1 = (\sum ||F_o| - |F_c|| / \sum |F_o|), wR_2 = \sum w(F_o^2 - F_c^2)^2 / \sum (F_o^2)^2)^{1/2}, s = (\sum w(F_o^2 - F_c^2)^2 / (n - p))^{1/2}.$$

side owing to the crystal problems and isotropic refinement of five disordered carbon atoms. Torsion angles, mean planes, and H-bonding were calculated by using PARST.¹²

Synthesis of Ligands and Copper(II) Complexes. The ligands N,N' -bis(2-benzimidazolylethyl)hexanediamide (ABHA) and N,N' -bis(2-benzimidazolymethyl)hexanediamide (GBHA) were prepared by adopting a method reported earlier.^{13,8} N -octyl derivatives of ABHA and GBHA were synthesized by modifying the procedure of Reed et al.¹⁴ Synthesis and characterization of the above ligands and their copper(II) complexes are available in the Supporting Information.

Oxidation of Alcohols. A 25 mL, two neck flask was fitted with a reflux condenser and an oxygen/nitrogen inlet. Copper complex [CuCl(O-GBHA)]Cl (23.5 mg; 0.0308 mmol) and chlorobenzyl alcohol (87.83 mg; 0.616 mmol) in 10 mL CH₂Cl₂ were stirred at room temperature for 10 min under nitrogen. Cumenyl hydroperoxide (0.088 mL; 0.616 mmol) was added and stirred for 20 min. At this point the d–d band of the copper complex was monitored (Figure 3). This was followed by raising the temperature of the reaction mixture to 40–45 °C on a water bath. Stirring was continued for 1–2 h. The reaction was monitored by visible spectroscopy, and it was found that the d–d band intensity drops to 50% of its original value, within a 30 min period (Figure 3), and subsequently remains constant for the remaining period of the reaction. No new band is generated during the reaction cycle in the region 300–1100 nm. The reaction mixture was further stirred for another 24 h at room temperature.

TLC of the reaction mixture show two major products that were visualized by spraying an ethanolic solution of 2,4-DNP (2,4-dinitrophenylhydrazine). The reaction products were finally separated by column chromatography using 10% ethyl acetate/hexane as eluant (one of them was identified as the corresponding aldehyde and the other as acetophenone). Identity of the aldehydes and

(9) Cescon, L. A.; Day, A. R. *J. Org. Chem.* **1962**, *27*, 581.

(10) Atomare, A.; Cascarano, G.; Giacobozzo, C.; Gualardi, A. *J. Appl. Crystallogr.* **1993**, *26*, 343.

(11) Sheldrick, G. M. *SHELXL-PC*, ver 5.05; Siemens Analytical Instruments Inc.: Madison, WI, 1994.

(12) Nardelli, M.; Parst, A. System of computer routines for calculating molecular parameters from results of crystal structure analysis. *Comput. Chem.* **1983**, *7*, 95.

(13) Gupta, M.; Das, S. K.; Mathur, P.; Cordes, A. W. *Inorg. Chim. Acta* **2003**, *353*, 197.

(14) McKee, V.; Zvagulis, M.; Dagdigian, J. V.; Patch, M. G.; Reed, C. A. *J. Am. Chem. Soc.* **1984**, *106*, 4765.

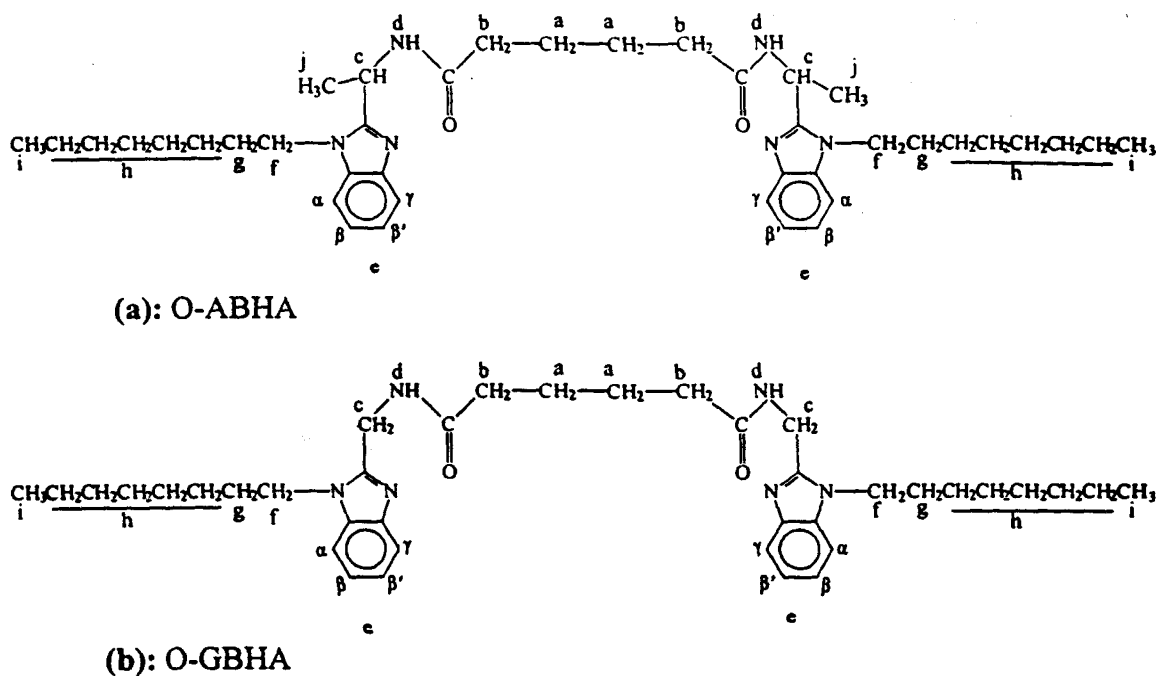


Figure 1. (a) O-ABHA and (b) O-GBHA.

acetophenone formed was confirmed by ^1H NMR of their respective DNP derivatives and are in confirmation with those reported in the literature. These data are provided in the Supporting Information section.

No products were obtained if the solution was not warmed to 40–45 °C for 1/2 h, and the oxidation state of copper(II) also does not change if the reaction mixture is not heated as above; this is confirmed by observing minimal change in d–d band intensity for such room-temperature solutions, for a period of several hours.

The percentage yields of the products obtained with the respective alcohols are shown in Table 3. Similar results were obtained using $[\text{CuCl}(\text{O-ABHA})]\text{Cl}$ and $[\text{Cu}(\text{NO}_3)(\text{O-GBHA})](\text{NO}_3)$ as catalysts.

Results and Discussion

Description of the Crystal Structure. A view, ORTEP view, and stereo drawing of the unit cell of the mononuclear $[\text{Cu}(\text{NO}_3)(\text{O-GBHA})]\text{NO}_3$ complex are shown in Figure 2a–c, respectively. The copper center in the complex has a tetragonally distorted octahedral environment. The six coordination comprises two imine nitrogens of the two benzimidazole rings, two amide oxygens of the ligand, and two oxygens of one of the nitrate anions. The carbonyl oxygen atom O2, nitrate oxygen atom O3, and the two benzimidazole imine nitrogen atoms N4 and N5 occupy the equatorial positions of the plane while the axial positions are occupied by another amide carbonyl oxygen atom O1 and nitrate oxygen atom O5 to generate a distorted octahedral geometry. Bond lengths (Table 2) show that the nitrate group behaves as a highly unsymmetrical bidentate chelating ligand, with Cu–O5 bond length 2.46 Å much longer than Cu–O3 bond length 2.074 Å. The bond angle $\angle\text{O3–Cu–O5}$ 55.1(8)° is in the range found for weakly coordinating bidentate ligands.¹⁵

(15) Hendriks, H. M. J.; Birker, P. J. M. W. L.; Rijn, J. V.; Verschoor, G. C.; Reedijk, J. *J. Am. Chem. Soc.* **1982**, *104*, 3607.

The Cu–N bond distances of 1.983 Å (Cu–N4) and 1.973 Å (Cu–N5) are found to be similar to those reported typically with imidazole/benzimidazole N-atoms in the equatorial plane.^{16a–c} Thus, the short distances in the present copper(II) complex probably reflect that the overall positive charge on the complex is not fully compensated by the unsymmetrical bidentate nitrate ligand as compared to those complexes with good coordinating anions.^{16d} The Cu–O bond distances of 2.020 Å (Cu–O2) and 2.212 Å (Cu–O1) are considerably longer than those reported in the literature for amide carbonyl coordination.¹⁷ The bond angles are quite close to the values expected for an octahedral structure except for $\angle\text{O1–Cu–O5}$ 156.5(7)° and O3–Cu–O5 55.1(8)°, which are on the smaller side. The distortion may be due to the combined results of the Jahn–Teller effects and the fixed bite size of the NO_3^- ion. The atoms O1, O2, O3, O5 and O2, O3, N4, N5 lie in approximate planes with maximum deviation of O5 being 0.05 Å in the former and O3 being 0.10 Å in the latter. The atoms O1, O5, N4, N5 lying in the third approximate plane have more deviations from it, the maximum being 0.5 Å for O5. These three planes are almost perpendicular to each other; the dihedral angles between the first and second and first and third are 85.5(3) and 86.7(3)°, respectively, whereas between

(16) (a) Prochaska, H. J.; Shwindinger, W. F.; Schwartz, M.; Burk, M. J.; Bernarducci, E.; Lalancette, R. A.; Potenza, J. A.; Schugar, H. J. *J. Am. Chem. Soc.* **1981**, *103*, 3446. (b) Prout, C. K.; Allison, G. B.; Rassottii, F. J. C. *J. Chem. Soc. A* **1971**, 3331. (c) Camerman, N.; Faweett, J. K.; Kruck, T. P. A.; Sarkar, B.; Camerman, A. *J. Am. Chem. Soc.* **1978**, *100*, 2690. (d) Jeffery, V.; Dagdigian, V. M.; Reed, C. A. *Inorg. Chem.* **1982**, *21*, 1332.

(17) (a) Lloret, F.; Julve, M.; Faus, J.; Ruiz, R.; Castro, I.; Mollar, M.; Levisalles, M. P. *Inorg. Chem.* **1992**, *31*, 784. (b) Frances, L.; Julve, M.; Real, J.; Faus, J.; Ruiz, R.; Mollar, M.; Castro, I.; Bois, C. *Inorg. Chem.* **1992**, *31*, 2925. (c) Lloret, F.; sletten, J.; Ruiz, R.; Julve, M.; Faus, J.; Verdager, M. *Inorg. Chem.* **1992**, *31*, 778. (d) Sangeetha, N. R.; Baradi, K.; Gupta, R.; Pal, C. K.; Manivannan, V.; Pal, S. *Polyhedron* **1999**, *18*, 1452.

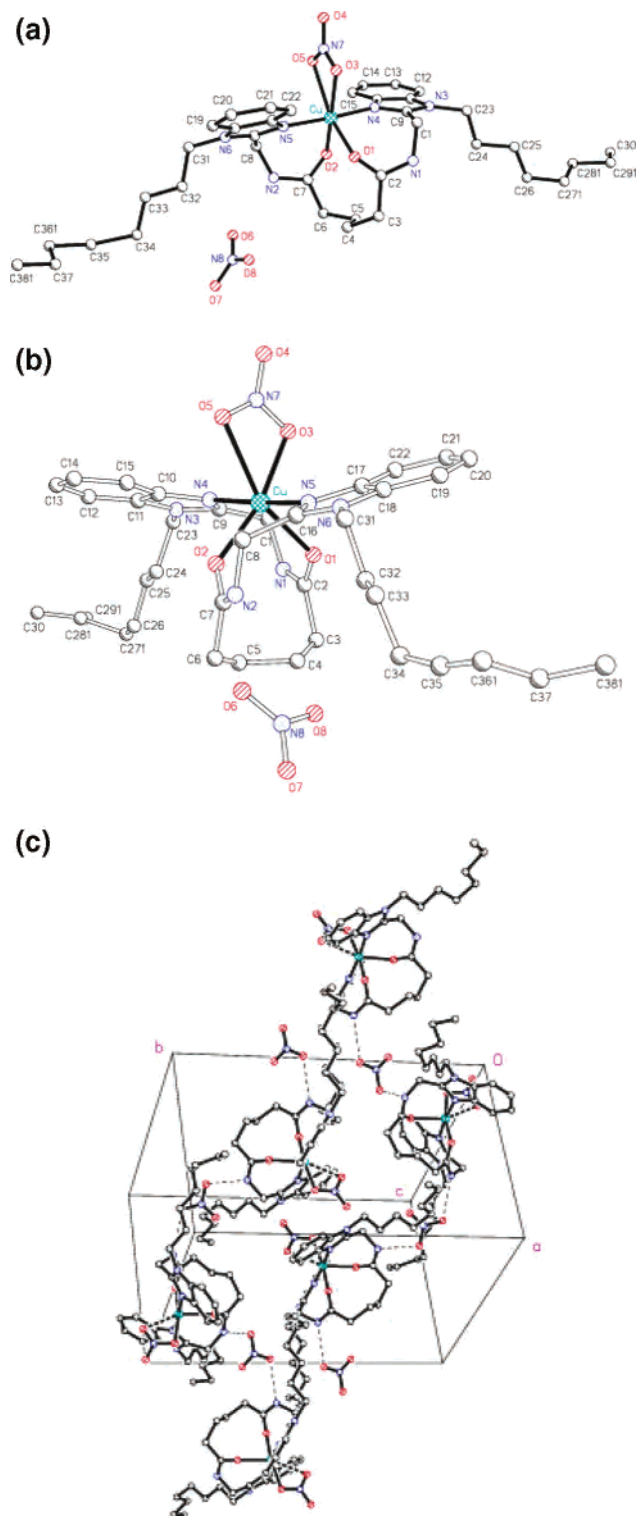


Figure 2. (a) View of $[\text{Cu}(\text{O-GBHA})(\text{NO}_3)](\text{NO}_3)$ showing the atomic numbering scheme. (b) ORTEP view of $[\text{Cu}(\text{O-GBHA})(\text{NO}_3)](\text{NO}_3)$ showing the rotation about the C3–C4–C5–C6 bond. (c) Stereo drawing of the unit cell contents of $[\text{Cu}(\text{O-GBHA})(\text{NO}_3)](\text{NO}_3)$ showing the packing and H-bonding interactions.

first and third is $76.9(4)^\circ$. Two benzimidazole rings are planar and have a dihedral angle of $29.4(3)^\circ$ with respect to each other. Torsion angles (Cu–N4–C10–C15, 8° ; Cu–N5–C17–C22, $6^\circ(3)$; also N4–C10–C15–C14, $179(2)^\circ$; N5–C17–C22–C21, $-178(2)^\circ$) show that the two benzimidazole

Table 2. Important Bond Lengths (Å) and Angles (deg)

Bond Lengths			
Cu–N(5)	1.973(12)	Cu–N(4)	1.983(12)
Cu–O(2)	2.020(12)	Cu–O(3)	2.074(18)
Cu–O(1)	2.212(15)	Cu–O(5)	2.46(2)
Bond Angles			
N(5)–Cu–N(4)	174.0(6)	N(5)–Cu–O(2)	94.6(5)
N(4)–Cu–O(2)	83.3(5)	N(5)–Cu–O(3)	91.8(5)
N(4)–Cu–O(3)	89.0(6)	O(2)–Cu–O(3)	165.8(7)
N(5)–Cu–O(1)	90.2(5)	N(4)–Cu–O(1)	95.4(6)
O(2)–Cu–O(1)	91.2(6)	O(3)–Cu–O(1)	101.4(8)
N(5)–Cu–O(5)	91.0(6)	N(4)–Cu–O(5)	84.6(6)
O(2)–Cu–O(5)	112.1(7)	O(3)–Cu–O(5)	55.1(8)
O(1)–Cu–O(5)	156.5(7)		

rings are projected in opposite directions to each other. The conformation of the chain joining the two benzimidazole rings may be defined as $\bar{g}aagaga\bar{a}g$. A kink at C3–C4–C5–C6 gives a spiral turn to the ligand, and it wraps around the metal ion in the form of a half-helix. The packing of the molecule shows an extensive H-bonding network; some of these interactions are shown in the packing diagram in Figure 2c. It involves intramolecular H-bonds between amide nitrogen N2 and O6 and N8 of the free nitrate group. The second amide nitrogen N1 is giving two strong intermolecular H-bonds with O7 and N8 of the symmetry-related uncoordinated nitrate group. Apart from these, there are a number of weak C–H \cdots O and C–H \cdots N H-bonding¹⁸ interactions involving both the nitrate ions and various methylene and phenylene carbons.

Electronic Spectroscopy and ¹HNMR. The electronic spectra of the ligands show two strong bands in the UV region at 277 and 284 nm. These bands are assigned to the π – π^* transition characterizing the benzimidazole group.¹⁹ The spectra of the complexes also show two strong bands at 275 and 283 nm corresponding to π – π^* transitions; the bands are slightly blue shifted with lowered extinction coefficient. A broad much less intense d–d band is observed in the region 720–820 nm. The low energy of d–d transition suggests a severely distorted tetragonal copper(II) complex, in the solution state.

The ¹HNMR spectra of the octylated ligand (O-ABHA) (Figure 1a) in CDCl₃ show signals for both aliphatic and aromatic protons. A doublet at 8.80 ppm arises due to amide NH protons d ($J = 7.74$ Hz). The CH proton c is found at 5.40 ppm as a multiplet ($J = 6.99$ Hz), coupled to adjacent amide NH and CH₃ protons j. Both these protons are downfield shifted as compared to bis(benzimidazolyl) diamide ligands.⁸ This is due to the deshielding effect of the CH₃ group on the carbon atom array. The aromatic protons e (α , β , β' , γ) are observed in the range of 7.2–7.7 ppm in the ratio 1:2:1 for α : β : β' : γ . N-octylation disturbs the normal AA'BB' type pattern commonly observed for benzimidazoles.⁸ The CH₂ protons a along with proton g give a multiplet at 1.65 ppm corresponding to eight protons while the CH₂ protons h and CH₃ protons j overlap to give a broad

(18) Desiraju, G. R.; Steiner, T. *The Weak Hydrogen Bond*; IUCr; Oxford Science Publications: Oxford, U.K., New York, 1999.

(19) Monzani, E.; Quinte, L.; Perotti, A.; Casella, L.; Gullotti, M.; Randaccio, L.; Geremia, S.; Nardil, G.; Faleschini, P.; Tabbi, G. *Inorg. Chem.* **1998**, *37*, 553.

single peak at 1.25 ppm (corresponding to 26 protons). The CH₃ protons i of the octyl chain give rise to a triplet at 0.80 ppm, due to coupling to adjacent CH₂ protons. The CH₂ protons b are found at 2.20–2.30 ppm, and protons f are found at 4.10–4.28 ppm. They are split into two doublets each. This can be explained on the basis of nonequivalence of the CH₂ protons because of a *N*-octyl chain along with asymmetric center in O-ABHA as compared to O-GBHA and ABHA. This is in keeping with similar effects reported earlier.²⁰

¹HNMR of the ligand O-GBHA is altered in comparison to O-ABHA. The amide NH proton d is now at 8.55 ppm as a triplet due to coupling with two methylene protons c (*J* = 4.8 Hz). The methylene protons c are now found at 4.60 ppm as a doublet (*J* = 5.4 Hz). Aromatic protons (α, β, β', γ) follow the pattern similar to O-ABHA. The CH₂ protons a do not merge with protons g in the aliphatic chain; rather they show up as separate peaks at 1.74 and 1.82 ppm, respectively. The CH₂ protons b and the N-CH₂ protons f are not split and are found at 2.4 and 4.08, respectively, as a triplet. The splittings in the ¹HNMR signals assigned to the ligand ABHA have been provided.

Cyclic Voltametry, IR, and Magnetic Studies. The cyclic voltammograms were recorded in dichloromethane solution containing 0.10 M TBAP as supporting electrolyte at a glassy carbon working electrode. Ferrocene was used as internal standard, and potentials are referenced to the ferrocenium/ferrocene (Fc⁺/Fc) couple. The cyclic voltammograms display a quasi-reversible wave at fairly anodic potentials. This is attributed to the change of copper(II) to copper(I). The absence of the reduction wave in the case of nitrate suggests that nitrate anion stabilizes the copper(II) oxidation state considerably relative to the chloride complex.

The free ligands O-ABHA and O-GBHA have characteristic IR bands at 1638 and 1645 cm⁻¹, respectively, assigned to amide I (ν_{C=O}). The bands in the range 1542–46 cm⁻¹ are assigned to amide II (ν_{C-N}), while the band between 1450 and 70 cm⁻¹ is assigned to ν_{C=N-C=N} stretching of the benzimidazole group, respectively. These bands are shifted by 10–20 cm⁻¹ in the complexes, thus, implying a direct coordination of the imine nitrogen and amide carbonyl to the metal site. Characteristic stretching frequencies for the coordinated anion are also observed. The nitrate complex shows two bands at 1383 and 827 cm⁻¹ due to ν_{O-N-O}_{sym} and ν_{O-N-O}_{antisym} stretching of the coordinated nitrate group.

The Evans²¹ method was used for the determination of magnetic susceptibilities. These were corrected using Pascal's constants.²² The μ_{eff} values obtained are found to be in the range for similar copper(II) complexes reported earlier.^{8,13}

Oxidation Studies. Products separated by column chromatography were quantitatively estimated using HPLC. A standard curve for each of the aldehydes was generated, and

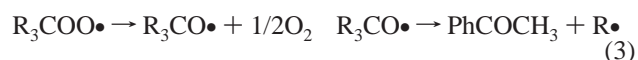
Table 3. Percentage Yield of Products Obtained on Oxidation of Various Alcohols Using [CuCl(O-GBHA)]Cl as Catalyst

substrate	products	
	ArCHO % yield (TON) ^a	PhCOCH ₃ % yield (TON) ^a
benzyl alcohol	39.0 (16)	28.0 (16)
4-chlorobenzyl alcohol	43.0 (18)	42.0 (23)
4-chlorobenzyl alcohol (under O ₂)	9.0 (4)	23.0 (12)
4-chlorobenzyl alcohol (with TBPH)	26.0 (11)	11.0 (6)
4-methylbenzyl alcohol	52.0 (18)	47.0 (26)
4-methoxybenzyl alcohol	65.0 (27)	28.0 (16)
4-nitrobenzyl alcohol	33.0 (13)	28.0 (16)
1-phenylethanol		66.0 (32)

^a TON = turnover number; error bar in the above yields was found to be on the order of 0.5–1.0% for a duplicate analysis.

the concentration of the unknown aldehyde was obtained with reference to the standard curve. On this basis, the percentage conversion and turnover number are reported in Table 3.

It is well established that, in the absence of protic solvent, the hydroperoxides are likely to cleave by homolysis reaction.²³ Further it has been reported that cumenyl hydroperoxide generates a cumylperoxy radical (R₃COO•) with metal ion complexes with concomitant change in oxidation state of the metal ion.²⁴ It is also established that cumylperoxy radicals decompose by a mechanism which finally generates acetophenone as one of the product.²⁵ The above two reaction sequences are presented as



It is assumed that the above reaction sequences are dominantly active in the present catalytic oxidation of alcohol. A spectral monitoring of the course of catalytic reaction shows a drop in d-d band intensity to almost half of its original value after thermally activating the reaction for nearly 30 min (Figure 3). This may imply the reduction of copper(II) to copper(I). However, there appears to be some structural change which takes place during the activation; the d-d band shifts by almost 30 nm (λ_{max}: 712 nm) to shorter wavelengths and a weak shoulder around 880 nm is also lost, when [CuCl(O-GBHA)]Cl complex is used as the catalyst. This possibly implies a loss of the axially bound atom in the complex leading to formation of an "active copper species".²⁶

In an attempt to identify the Cu(II) species that may be active in the peroxide-dependent oxidation of aryl alcohols, a sample of Cu(II) species (which formed after the reaction

(20) Jackman, L. M.; Sternhall, S. *Application of Nuclear Magnetic Resonance Spectroscopy in Organic Chemistry*; Pergamon Press: London, 1969; Vol. 5, Chapter 5-2, p 377.

(21) Evans, D. F. *J. Chem. Soc.* **1959**, 2003.

(22) Drago, R. S. *Physical Methods in Chemistry*; Saunders: Philadelphia, PA, 1977; Chapter 11, p 413.

(23) (a) Chin, D.; La Mar, G. N.; Balch, A. L. *J. Am. Chem. Soc.* **1980**, *102*, 5945. Balch, A. L. Private communication. (b) Arasasingham, R. D.; Balch, A. L.; Latos-Grazynski, L. *J. Am. Chem. Soc.* **1987**, *109*, 5846.

(24) Fukuzumi, S.; ONO, Y. *Bull. Chem. Soc. Jpn.* **1979**, *52*, 2 (8), 2255.

(25) Fukuzumi, S.; ONO, Y. *J. Chem. Soc., Perkin Trans.* **1977**, 2, 622.

(26) (a) Palaniandavar, M.; Pandiyan, T.; Lakshminarayanan, M. *J. Chem. Soc., Dalton Trans.* **1995**, 457. (b) Nonoka, Y.; Tokh, T.; Kida, S. *Bull. Chem. Soc. Jpn.* **1974**, 2, 312.

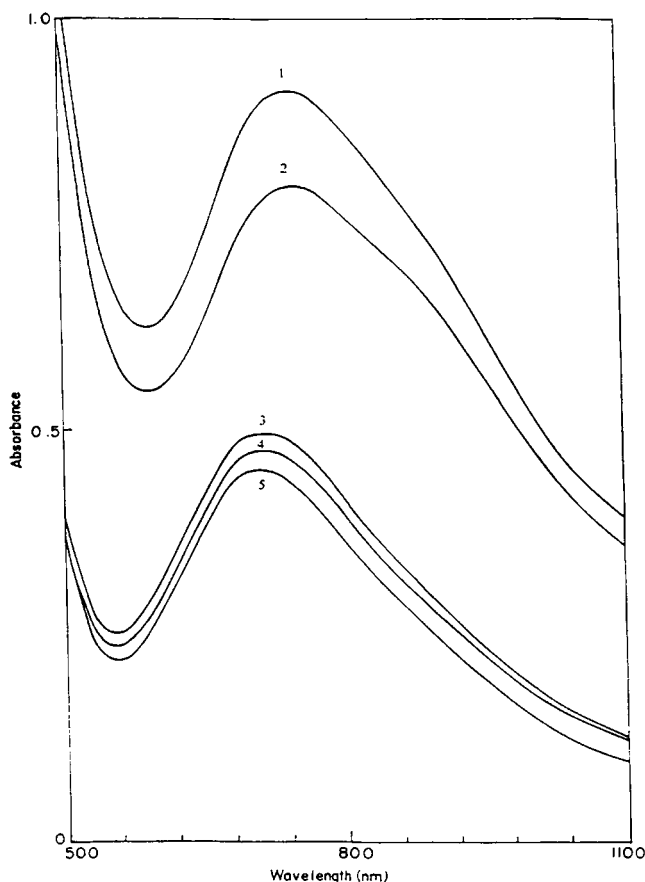


Figure 3. Curve 1: d-d band spectrum of a reaction mixture (0.0308 mmol of $\text{CuCl}(\text{O-GBHA})\text{Cl}$, 0.616 mmol of 4-chlorobenzyl alcohol, 0.616 mmol of cumenyl hydroperoxide) at the time of mixing. Curves 2-4: d-d band spectra of a reaction mixture after every 10 min of heating. Curve 5: d-d band spectrum of a reaction mixture 1 h after the initiation of reaction.

was thermally activated for 30 min in the presence of substrate and cumenyl hydroperoxide) was isolated and EPR of this sample was taken in CH_2Cl_2 at liquid- N_2 temperature. For a comparison, the EPR of the original complex $[\text{CuCl}(\text{O-GBHA})\text{Cl}]$ utilized in this reaction as a catalyst was also taken in the same solvent and at liquid- N_2 temperature. A comparison of the EPR spectra of the two species indicates that there is slight variation in their respective g -values; however, they follow the order $g_{\parallel} > g_{\perp} > 2.0023$, implying a $d_{x^2-y^2}$ ground state. There are, however, changes in the hyperfine coupling constants ($[\text{CuCl}(\text{O-GBHA})\text{Cl}]$ prior to reaction, $g_{\parallel} = 2.40$, $g_{\perp} = 2.12$, and $A_{\parallel} = 120$ G; $[\text{CuCl}(\text{O-GBHA})\text{Cl}]$ after the reaction, $g_{\parallel} = 2.34$, $g_{\perp} = 2.09$, and $A_{\parallel} = 135$ G). The $g_{\parallel}/10^{-4}A_{\parallel}$ index is 200 for the original complex while it is 173 for the active species. This implies that the active species is more planar relative to the starting complex.²⁷ This relative planarity may result due to the relieving of strain in the complex caused by the loss of the axially bound atom in the "active-copper species".

The role of molecular oxygen was also studied by allowing a slow stream of O_2 during the oxidation reaction catalyzed by the $[\text{CuCl}(\text{O-GBHA})\text{Cl}]$ complex. The change observed in the d-d band of the catalyst is depicted in Figure 4a. It

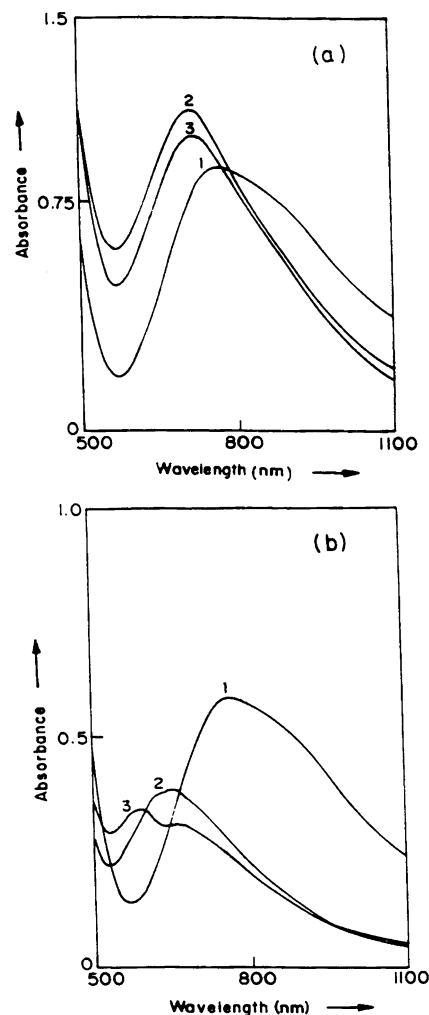


Figure 4. (a) Curve 1: d-d band spectrum of a reaction mixture (0.0308 mmol of $[\text{CuCl}(\text{OGBHA})\text{Cl}]$, 0.616 mmol of 4-chlorobenzyl alcohol, 0.616 mmol of cumenyl hydroperoxide) under O_2 at the time of mixing. Curve 2: d-d band spectrum of a reaction mixture 1 h after the initiation reaction. (b) Curve 1: d-d band spectrum of a reaction mixture (0.0308 mmol of $[\text{CuCl}(\text{OGBHA})\text{Cl}]$, 0.616 mmol of 4-chlorobenzyl alcohol, 0.616 mmol of cumenyl hydroperoxide, 0.308 mmol of TBPH) at the time of mixing. Curve 2: d-d band spectrum of a reaction mixture after 30 min of heating. Curve 3: d-d band spectrum of a reaction mixture 1 h after the initiation of reaction.

is found that the active-copper species with a $\lambda_{\text{max}} \sim 712$ nm is again generated, but in this case there is no drop in the absorbance of the d-d band of the catalyst; rather, there is slight increase in the absorbance. This implies a higher extinction coefficient of the d-d band for the active-copper(II) species relative to the starting complex. Further, the added molecular oxygen competes strongly with step 2 of the proposed reaction cycle and keeps most of the copper in the oxidized state. This has a direct impact on the yields of the two products, viz. aldehyde and acetophenone, that drop dramatically; the aldehyde yield decreases by 80% while the acetophenone by 46% (Table 3), indicating severe competition by oxygen in steps 2 and 3 of the reaction cycle.

The generation of cumylperoxyl radicals during the course of the present reaction is confirmed by the identification of acetophenone as one of the reaction products. Further, when

(27) Batra, G.; Mathur, P. *Inorg. Chem.* **1992**, *31*, 1575.

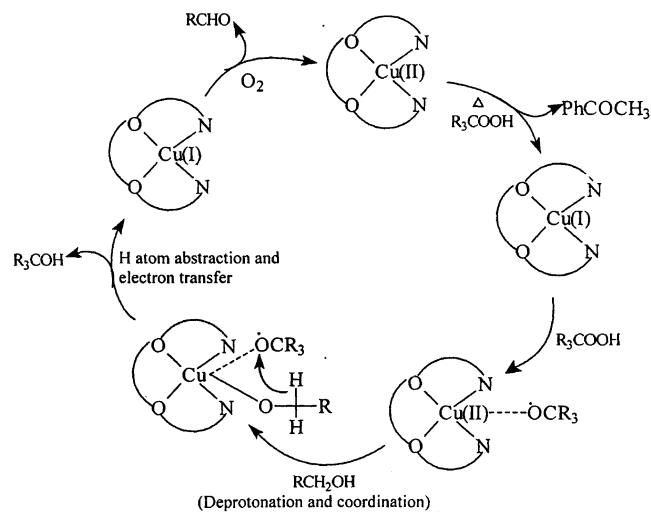


Figure 5. Proposed catalytic reaction cycle.

a radical trap like 2,4,6-tri-*tert*-butylphenol (0.308 mmol, TBPH) is included in the reaction mixture and the reaction is carried out as indicated under Oxidation of Alcohols in the Experimental Section (with vigorous exclusion of oxygen), it is found that a new band at ~ 640 nm generates after the reaction has been thermally activated for 30 min. This supports the formation of the stable 2,4,6-tri-*tert*-butylphenoxy radical²⁸ via the oxidation of TBPH by cumylperoxyl radicals (Figure 4b).

The yield of the aldehyde and acetophenone obtained after workup of the reaction indicates a drop of 40% in the yield of the aldehyde while a drop of 74% is found for the ketone (Table 3). This implies that the presence of the radical trap severely inhibits step 3 relative to step 1 of the proposed reaction cycle. This further justifies the presence and the utilization of cumylperoxyl radical in the oxidation of 2,4,6-tri-*tert*-butylphenol to the phenoxy radical.

The proposed catalytic reaction cycle is depicted in Figure 5. This reactivity is reminiscent of the functioning of galactose oxidase.

Acknowledgment. We gratefully acknowledge financial support from the Department of Science and Technology of India (Project No. SR/S1/IC-35/03). We are also thankful to Prof. S. M. S. Chauhan, Department of Chemistry, University of Delhi, Delhi, India, for allowing us to use the HPLC facilities.

Supporting Information Available: Text describing the synthesis and characterization of ligands and complexes, a table of ^1H NMR data for the DNP derivatives isolated for the aldehydic and ketonic products, and atomic coordinates and equivalent isotropic displacement parameters (Table S1) and bond lengths and angles (Table S2) for the complex $[\text{Cu}(\text{NO}_3)(\text{O-GBHA})](\text{NO}_3)$. This material is available free of charge via the Internet at <http://pubs.acs.org>.

IC0302884

(28) Cook, C. D.; Norcross, B. E. *J. Am. Chem. Soc.* **1958**, *81*, 1176.